Journal of Molecular Catalysis A: Chemical 300 (2009) 89–97

Contents lists available at ScienceDirect

Journal of Molecular Catalysis A: Chemical

journal homepage: www.elsevier.com/locate/molcata

Homogeneous and heterogeneous olefin epoxidation catalyzed by a binuclear Mn(II)Mn(III) complex

Silvana T. Castaman[a], Shirley Nakagaki[a], Ronny R. Ribeiro[a], Kátia J. Ciuffi[b], Sueli M. Drechsel[a,*]

[a] Departamento de Química, Universidade Federal do Paraná, C.P. 19081, CEP 81531-990 Curitiba, PR, Brazil
[b] Universidade de Franca, Av. Dr. Armando Salles Oliveira 201, 14404-600 Franca, SP, Brazil

ARTICLE INFO

Article history:
Received 20 May 2008
Received in revised form 23 October 2008
Accepted 23 October 2008
Available online 5 November 2008

Keywords:
Manganese
Sol–gel
Silica
EPR
Supported catalyst
Catalysis
Oxidation

ABSTRACT

The synthesis and characterization of a binuclear carboxylated bridged manganese complex containing the heptadentate ligand *N*,*N*′-bis(2-hydroxybenzyl)-*N*,*N*′-bis(2-methylpyridyl)-2-ol-1,3-propanediamine (H_3bbppnol) is reported. This complex was characterized by elemental analysis; infrared, electronic (UV–vis) and EPR spectroscopy; and conductivity measurements. The complex was immobilized on silica by either adsorption or entrapment via a sol–gel route. The obtained solids were characterized by thermogravimetric analyses (TG and DSC), UV–vis and infrared spectroscopy, and X-ray diffraction. The catalytic performance of the binuclear manganese complex in epoxidation reactions was evaluated for both homogeneous and heterogeneous systems. The catalytic investigation revealed that the complex performs well as an epoxidation catalyst for the substrates cyclohexene (26–39%) and cyclooctene (29–74%). The solids containing the immobilized complex can be recovered from the reaction medium and reused, maintaining good catalytic activity.

© 2008 Elsevier B.V. All rights reserved.

1. Introduction

Oxygenation of organic substrates has been extensively studied, and hydrocarbon oxidation is especially interesting because of the industrial importance of this type of reaction. Among such oxidation reactions, epoxidation is extremely important for the preparation of highly functionalized organic compounds [1–3].

Transition metal complexes have attracted a lot of attention from researchers as possible oxidation catalysts for the selective oxidation of hydrocarbons in mild conditions [4–9]. In fact, there are countless studies on iron and manganese complexes as oxidation catalysts because these metals are less damaging to the environment compared with many other transition metal species [8,10–12].

Manganese 1,4,7-trimethyl-1,4,7-triazacyclononane complexes, firstly described by Wieghardt et al. [13], are highly active for catalytic oxidation in homogeneous and heterogeneous media [14–16].

The binuclear manganese(IV) complex $[Mn_2^{IV}(\mu\text{-}O)_3(Me_3\text{-}tacn)_2](PF_6)_2$ is a highly active oxidation catalyst [17,18]. Feringa and co-workers [19] have reported that the use of carboxylic acids at co-catalyst levels improves the selectivity of the binuclear manganese(IV) Me_3-tacn compound toward *cis*-dihydroxilation and epoxidation. They have confirmed that the reaction control arises from the *in situ* formation of carboxylate-bridged dinuclear complexes.

The dimeric Mn_2(2-OHsalpn)$_2$ μ-alkoxo species prepared by Pecoraro and co-workers [20] have been isolated as the binuclear structure containing two μ-alkoxo bridges; their coordination sphere is completed by two ligand molecules. These species may also exist in the solvated form, thus leading to an unsaturated coordinative structure where one of the alkoxo groups remains monocoordinated to the metal, leaving one position free for the approach of reactive ligands. The interaction of these systems with oxidant molecules has been reported.

In the present work, the synthesis and characterization of the binuclear carboxylated bridged manganese complex containing the heptadentate ligand *N*,*N*′-bis(2-hydroxybenzyl)-*N*,*N*′-bis(2-methylpyridyl)-2-ol-1,3-propanediamine (H_3bbppnol) **(1)** is reported (Fig. S1—supplementary material) [21]. The heptadentate ligand contains an alcohol group between the two halves of the molecule, which induces formation of a binuclear manganese structure. Besides the coordination sites available for the ligand, each manganese atom can bind other molecules, such as carboxylate, water or other solvent molecules. These open sites can also bind an oxidant molecule, thus forming an active intermediate species

* Corresponding author at: Departamento de Química, Universidade Federal do Paraná, Centro Politécnico, Jardim das Américas, C.P. 19081, 81531-990 Curitiba, Brazil. Tel.: +55 41 3361 3299; fax: +55 41 3361 3186.
E-mail address: sueli@quimica.ufpr.br (S.M. Drechsel).

1381-1169/$ – see front matter © 2008 Elsevier B.V. All rights reserved.
doi:10.1016/j.molcata.2008.10.037

for the oxidation of organic substrates, like the ones observed for the Me_3-tacn systems. An alternative coordination site for the oxidant molecule is the μ-alkoxo bridge, which can also undergo the rearrangement proposed by Pecoraro and co-workers [20].

The catalytic performance of complex **1** in both homogeneous and heterogeneous media was evaluated in epoxidation reactions. The complex was immobilized on silica gel by either adsorption or via a sol–gel process using TEOS [22].

2. Experimental

2.1. Materials

All chemicals were of analytical and spectroscopy grade and were purchased from Aldrich, Sigma, Acros or Merck. Silica gel (Merck 70-230 mesh ASTM) was activated at 100 °C under vacuum for 6 h. Iodosylbenzene (PhIO) was synthesized by hydrolysis of iodosylbenzenediacetate [23]. The solid was carefully dried under nitrogen atmosphere and kept at 5 °C. The purity was periodically controlled by iodometric assay [24].

The ligand *N*,*N*′-bis(2-hydroxybenzyl)-*N*,*N*′-(2-methylpyridyl)–1,3-propanediamine-2-ol (H_3bbppnol) was synthesized and characterized according to a previously published procedure [21]. The structural formula of H_3bbppnol is shown in Fig. S1 (supplementary material). (^{1}H NMR (δ $CDCl_3$): 8.9 (m, 2H, two phenolic protons); 6.9–8.3 (m, 16H, phenyl and py); 3.9–4.4 (m, 9H, N–CH_2–R and R_2–CH–OH); 2.6–3.0 (d, 4H, (N–CH_2)$_2$).)

2.2. Instrumentation

FTIR spectra were recorded on a Biorad 3500 GX spectrophotometer in the 400–4000 cm^{-1} range, using KBr pellets. KBr was crushed with a small amount of the solid, and the spectrum was collected with a resolution of 4 cm^{-1} and accumulation of 32 scans. UV–vis spectra were recorded in the 200–800 nm range on an HP 8452A Diode Array Spectrophotometer. A cell with a path length of 1 cm was employed in all the analyses. Solid UV–vis spectra were recorded in the 200–800 nm range on an NIR Diode Array spectrophotometer, Perkin-Elmer Lambda 19, using KBr pellets. Elemental analyses were determined on the CHN Perkin-Elmer 2400 analyzer. Metal contents were measured using a Shimadzu Model 8100 Atomic Absorption Spectrometer graphite stove. Solid-state magnetic susceptibilities of powdered samples were measured with a Faraday-type magnetometer in 298 K. Cyclic voltammetry and coulometry were performed on an EG&G Princeton PARC 273A Potentiostat (working electrode: glassy carbon for voltammetry and a platinum grid for coulometry, reference electrode: Ag/AgCl, counter electrode: platinum, and support electrolyte: tetrabutylammonium hexafluorophosphate). The molar conductivities of the complexes in acetonitrile solutions were measured on a Digimed D-20 equipment (platinum electrode K = 1 cm^{-1}). CW-EPR experiments were performed at X band using a Bruker ESP-300E spectrometer equipped with a rectangular TE_{102} resonator (Bruker 4102 ST). The experiments were carried out at liquid nitrogen boiling temperature (77 K) using an on-top reservoir quartz finger dewar. All samples were put in 3 mm inner diameter EPR quartz tubes. CW-EPR spectra were simulated using the EasySpin software package for Matlab® platform [25]. The search for the best parameter set was optimized using *simplex* algorithm. For the XRD measurements, self-oriented films were placed on neutral glass sample holders. The measurements were performed in the reflection mode using a Shimadzu XRD-6000 diffractometer operating at 40 kV and 40 mA (Cu Kα radiation λ = 1.5418 Å), with a dwell time of 2° min^{-1}. A Shimadzu GC-17A gas chromatograph equipped with a DBWAX column (stationary phase: polyethyleneglycol), coupled to an integrator Shimadzu CBM-102 (with a flame ionization detector), was used for quantitative analysis in the oxidation experiments. Thermal analyses were carried out using a TGA Instruments Shimadzu TGA-50 thermogravimetric analyzer equipped with a platinum cell and a 50 mL min^{-1} gas flow.

2.3. Synthesis of [Mn_2(bbppnol)(μ-AcO)$_2$] (**1**)

Triethylamine (6.0 mmol) and $Mn(AcO)_2{\cdot}4H_2O$ (4.0 mmol) were added to a H_3bbppnol methanol solution (2.0 mmol). The deep red-brown solution was heated to 50 °C and magnetically stirred for 30 min. A brown precipitate was obtained after the solution was cooled down. The solid was filtered off and washed with cold ether. Yield: 38%. Anal. calc. for $C_{33}H_{37}N_4O_7Mn_2$ (709.44 g mol^{-1}): C, 53.16; H, 5.27; N, 7.51; Mn 15.48. Found: C, 53.37; H 4.85; N, 7.5; Mn 15.05. UV–vis acetonitrile solution: λ, nm (ε, mol^{-1} L cm^{-1}) 394 (1710) 496 (980).

2.4. Immobilization of complex **1** on silica (**Si-1**)

Silica gel (0.60 g) was suspended in acetonitrile (5 mL) under mild magnetic stirring. Complex **1** (1.44×10^{-4} mol ≈ 0.102 g) diluted in a minimum amount of acetonitrile was added to the suspension under reflux (85 °C). After 6 h of reaction, the resulting solid **(Si-1)** was filtered off and washed exhaustively with acetonitrile in a Soxhlet extractor for 6 h. The color of the silica became deep red brown. The solution obtained after **Si-1** was filtered off at the end of the immobilization reaction, together with the washings from the Soxhlet procedure, was quantitatively analyzed by UV–vis spectroscopy, in order to determine the amount of complex **1** that remained in the reaction solution and thus calculate the amount of **1** that was effectively immobilized on silica. **Si-1** was dried at room temperature for 24 h and characterized by UV–vis and IR spectroscopy, thermogravimetric analysis, and X-ray diffraction (XRD).

2.5. Heterogenization of **1** on silica by the sol–gel process (**SG-1**)

The **SG-1** catalyst was prepared by adaptation of the methodology described by Stober [22,26], through hydrolysis of TEOS in ethanol, in the presence of NH_4OH as catalyst, as well as 1.9×10^{-5} mol of **1**. The matrix was also prepared in the absence of **1** for use in control reactions. The reaction mixture was kept at 40 °C under magnetic stirring for 30 min. The precipitated solid **SG-1** was extensively washed with water, methanol, and acetonitrile. To determine the amount of **1** that was immobilized in TEOS, the amount of the manganese complex that remained in the reaction solution and combined washings was quantified by UV–vis spectroscopy. After the washing procedure, **SG-1** was dried at room temperature for 24 h.

2.6. Oxidation of cyclooctene and cyclohexene by iodosylbenzene (PhIO) catalyzed by **1** (homogeneous catalysis), and **Si-1** and **SG-1** (heterogeneous catalysis)

Catalytic oxidation reactions were carried out in a 2 mL thermostatic glass reactor equipped with a magnetic stirrer, inside a dark chamber. In a typical reaction employing the heterogeneous catalyst, **Si-1** (5 mg) or **SG-1** (40 mg), and the solid iodosylbenzene were degassed with argon for 10 min inside a 2 mL vial. The solid mixture was suspended in 0.35 mL of solvent (dichloromethane/acetonitrile (1:1)), and then 0.15 mL of the substrate, cyclooctene or cyclohexene, was added, resulting in a **Si-1** or **SG-1**/oxidant/substrate molar ratio of 1:10:1000. The oxidation reaction was carried out for a certain time (1 and 6 h), under magnetic stirring. Sodium sulfite

was added after the reaction, in order to eliminate the remaining iodosylbenzene. The solid catalyst was separated from the reaction products present in the solution by centrifugation and was then exhaustively washed with dichloromethane and acetonitrile. All the extracted solution and supernatant were transferred to a volumetric flask and analyzed by gas chromatography. Product yields were based on PhIO and were calculated by the internal standard method. The solid catalyst was thoroughly washed and dried for reuse in another reaction. In order to check the reproducibility of the determinations, all reactions were repeated two to three times because a micromethod was employed to measure catalytic activities. Only average results are reported. The same procedure was followed for the control reactions using: (a) the substrate only, (b) substrate + oxidant, and (c) substrate + oxidant + silica. The procedure for the reactions carried out in homogeneous medium was similar to that employed for the heterogeneous catalysis. A solution of **1** was prepared using dichloromethane/acetonitrile 1:1 as solvent ($\approx 1 \times 10^{-6}$ mol L^{-1}), and the same catalyst/oxidant/substrate molar ratio of 1:10:1000 was used. Quantitative analysis of the reaction products was carried out by gas chromatography (GC), using the internal standard method.

3. Results and discussion

3.1. Synthesis and characterization of [Mn_2(bbppnol)(μ-AcO)$_2$] (**1**)

The heptadentate ligand H_3bbppnol, which has an alcohol group between the nitrogen atoms of propanediamine, facilitates the formation of binuclear compounds with the alkoxo group bridging the metal atoms [8,21]. The presence of carboxylate groups in the metal salt employed in the synthesis promotes the formation of acetate bridges, thus closing the coordination sphere of the manganese atoms. The molar conductivity measured for a 1×10^{-3} mol L^{-1} acetonitrile solution of **1** is 32 S cm^{-2} mol^{-1}, which indicates that it is a non-electrolyte [27]. The infrared spectra of **1** on KBr disks displays strong bands at 1585 and 1448 cm^{-1}, attributed to the acetate groups. The difference between the symmetric and asymmetric bands (Δ = 137 cm^{-1}) is indicative of bridging modes of the carboxylate groups [28]. The electronic spectrum of the complex is similar to those observed for manganese(III) complexes containing phenolate ligands, and the intense bands are attributed to LMCT pπ (phenolate) → dπ^* (Mn^{III}) [29,30]. The EPR spectrum of an acetonitrile solution of **1** in 10 K has 20 lines in g = 2.0, typical of a binuclear mixed-valence $Mn^{III}Mn^{II}$ complex (Fig. S2—supplementary material) [31–37].

Powdered sample **1** magnetic susceptibility measurement at 293 K (Faraday method) has shown an effective magnetic moment (μ_{eff}) of 5.34μ_{eff}/μ_B per manganese center pointing to 4.43 electrons per Mn. These data are coherent with a $Mn^{III}Mn^{II}$ center.

The following peaks are observed in the cyclic voltammogram of **1**: E_1 = +1.3 V (ΔE_p = 122 mV), E_2 = +0.25 V (ΔE_p = 90 mV), and E_{3c} = −0.5 V *vs* Ag/AgCl (E_1 = +0.8 V, E_2 = −0.25 V, and E_{3c} = −1.0 V *vs* Fc^+/Fc), attributed to the redox processes $Mn^{IV}Mn^{III}$–$Mn^{III}Mn^{III}$–$Mn^{III}Mn^{II}$–$Mn^{II}Mn^{II}$. The observation of three oxidation processes indicates that the coordination environment formed by the ligand and the acetate groups promotes accessibility of the metal centers to various redox states. This fact may be useful in catalytic reactions like the oxidation of organic substrates.

The redox behavior of **1** is similar to that observed for the binuclear complex with a phenol group bridging the manganese centers synthesized by Lomoth and co-workers [31,38]. The Lomoth complex was isolated as a $Mn^{III}Mn^{III}$ complex with II,II → II,III and II,III → III,III potentials at −0.3 and 0.0 V *vs* SCE. The potentials of the redox processes are closer than the potentials observed for **1** (−0.5 and +0.25 V). This shows that the mixed-valent specie in **1** has larger stability domain than the analogous phenolate bridged complex. The potential difference between the oxidative and reductive electron transfer for **1** is larger by ca. 450 mV in comparison to the Lomoth complex (ΔE = 750 mV *vs* ΔE = 300 mV) which conduces to a larger comproportionation constant K_{com} of 4.8×10^{12} *vs* 1.2×10^5 based on the equation.$[Mn^{II}Mn^{II}] + [Mn^{III}Mn^{III}] \leftrightarrow 2[Mn^{III}Mn^{II}]$, $\Delta E = \left(\frac{RT}{nF}\right) \ln K_{com}$. In the coulometry experiments, 0.97 electrons are transferred during the oxidation process at +0.5 V *vs* Ag/AgCl, which indicates formation of the $Mn^{III}Mn^{III}$ species. The cyclic voltammetry profile of the solution obtained after the oxidation process is the same as that of the precursor complex. The electronic spectrum of the obtained solution displays bands at 506 and 684 nm, which are more intense than those observed for the mixed valence species $Mn^{II}Mn^{III}$. A spectroelectrochemical experiment for the oxidation process (Fig. S3—supplementary material) also gives evidence of the increase in the absorbance of the bands observed for **1**. These results give an indication that the oxidized $Mn^{III}Mn^{III}$ complex has the same structure as **1**.

The techniques used for the characterization of **1** support the binuclear structure proposed for it, with the alcohol and carboxylate groups bridging the two metal centers (Fig. 1).

3.2. Characterization of ***Si-1*** and ***SG-1***

Loading of complex **1** in the solids was determined by measuring the difference between the absorbance of the complex in the solution prepared before the immobilization process and the absorbance of the solution and combined washings from the Soxhlet procedure obtained after complex immobilization. The catalyst loadings in **Si-1** and **SG-1** were 2.7×10^{-4} mol g^{-1} (19.2% weight) and 3.4×10^{-5} mol g^{-1} (2.6% weight), respectively.

The infrared spectra of the heterogeneous catalysts **Si-1** and **SG-1** are very similar and their profile is typical of the silica matrix. Strong Si–O stretching vibrations are observed at 460 cm^{-1}, which corresponds to δ(Si–O–Si). The band at 960 cm^{-1} is due to ν(Si–OH), while the band 1090 cm^{-1} is assigned to ν_{as}(Si–O–Si) [28,39]. The absence of bands typical of the manganese complex can be attributed to the low loading of **1** in the matrices.

The reflectance electronic spectrum of the **Si-1** displays bands at 380, 480 and 520 nm, which is very similar to the spectrum obtained for **1** in the solid state (380, 480 and 530 nm) (Fig. 2). The similarity between the UV–vis spectra of **Si-1** and complex **1** suggests that the immobilization process does not alter the basic structure of the manganese compound. As for the reflectance electronic spectrum of **SG-1**, it displays bands at 380 and 480 nm, so its profile is similar to that of **1**. However, the absence of the band around 520 nm suggests that some modifications to the structure of **1** take place during the entrapment process, although the basic structure is maintained. The basic medium used in the preparation of the gel solid may have promoted substitution of the acetate

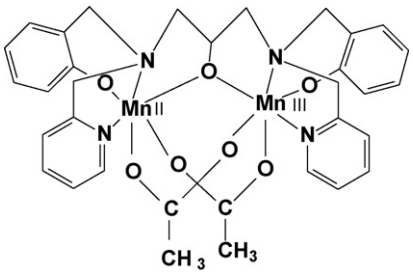

Fig. 1. Proposed structure for complex **1**.

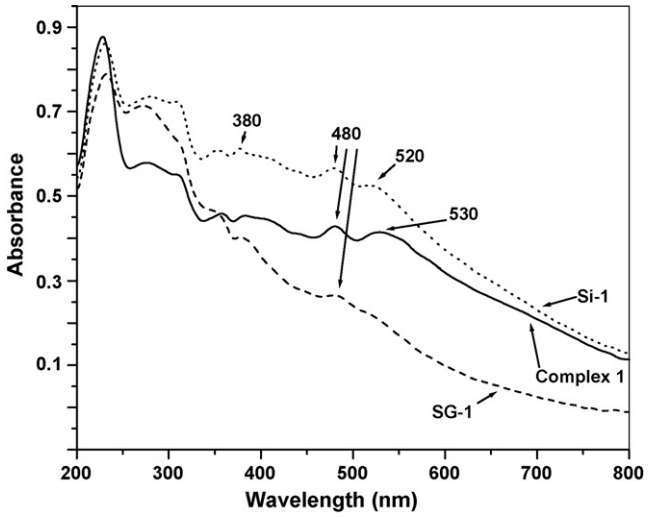

Fig. 2. Reflectance electronic spectrum of the solids **1**, **Si-1** and **SG-1** in KBr pellets.

bridges in **1** for other groups like hydroxo, which are also present in the solid structure. However, the low loading of **1** in this solid poses some difficulty to the correct interpretation of the spectrum profile.

The X-ray powder diffraction (XRD) patterns of the silica and sol–gel blank (without catalyst) and **Si-1** and **SG-1** were recorded at 2– values ranging between 3° and 60°. In all the cases, the typical diffraction pattern of amorphous samples was observed. Analysis of the diffractograms revealed that **Si-1** and **SG-1** are structurally similar to the corresponding matrices without any catalyst. Thus, the immobilization and entrapment processes do not change the amorphous diffraction pattern of the silica support.

Thermogravimetric analyses (TGA and DSC) were carried out under air for **1** (Fig. 3a), **SG-1** (Fig. 3b), and **Si-1** (Fig. 3c). Analyses for the silica obtained by sol–gel (**SG**) and pure silica (**Si**) were also performed. There is a mass loss between 25 °C and 150 °C for all the analyzed solids, which corresponds to the loss of water molecules weakly bound to the materials. This loss varies between 4.7% of the total mass for **Si-1** (Fig. 3c) to 8.4% for pure silica (**Si**). As for the thermal analysis of the pure complex **1** (Fig. 3a), there is a total weight loss of 75.20% between 150 °C and 1000 °C due to combustion of organic material, with formation of MnO_2. The main exothermic event corresponding to this weight loss takes place at around 400 °C.

Concerning **SG-1** (Fig. 3b), an exothermic weight loss is also observed around 400 °C, compatible with the loss of complex **1**. This suggests that it is really possible to entrap **1** in the silica obtained by the sol–gel process. The peak at 400 °C in Fig. 3b is less intense than that observed in the case of complex **1** (Fig. 3a) because of the low loading of **1** in **SG-1**. Indeed, the thermogram in Fig. 3b shows an exothermic weight loss between 150 °C and 450 °C corresponding to 2.2% of the **SG-1** mass. If we consider the loading of **1** in **SG-1** (3.61×10^{-5} mol of complex 1/g of silica gel), this value is consistent with the mass percent of **1** (2.56%) in **SG-1**.

As for **Si-1** (Fig. 3c), one intense peak at 380 °C is also observed, which can be assigned to loss of the immobilized complex **1**. This loss is around 14%, in agreement with the loading of complex **1** in **Si-1** (2.72×10^{-4} mol/g, which corresponds to 19% of **1** immobilized on silica). The differences in the thermal processes regarding the pure complex **1**, and the two solids **SG-1** and **Si-1** may be attributed to the different interactions taking place between **1** and the solid matrices. In fact, complex **1** may be adsorbed on the solid surface in **Si-1**, while it is confined inside the pores in **SG-1**.

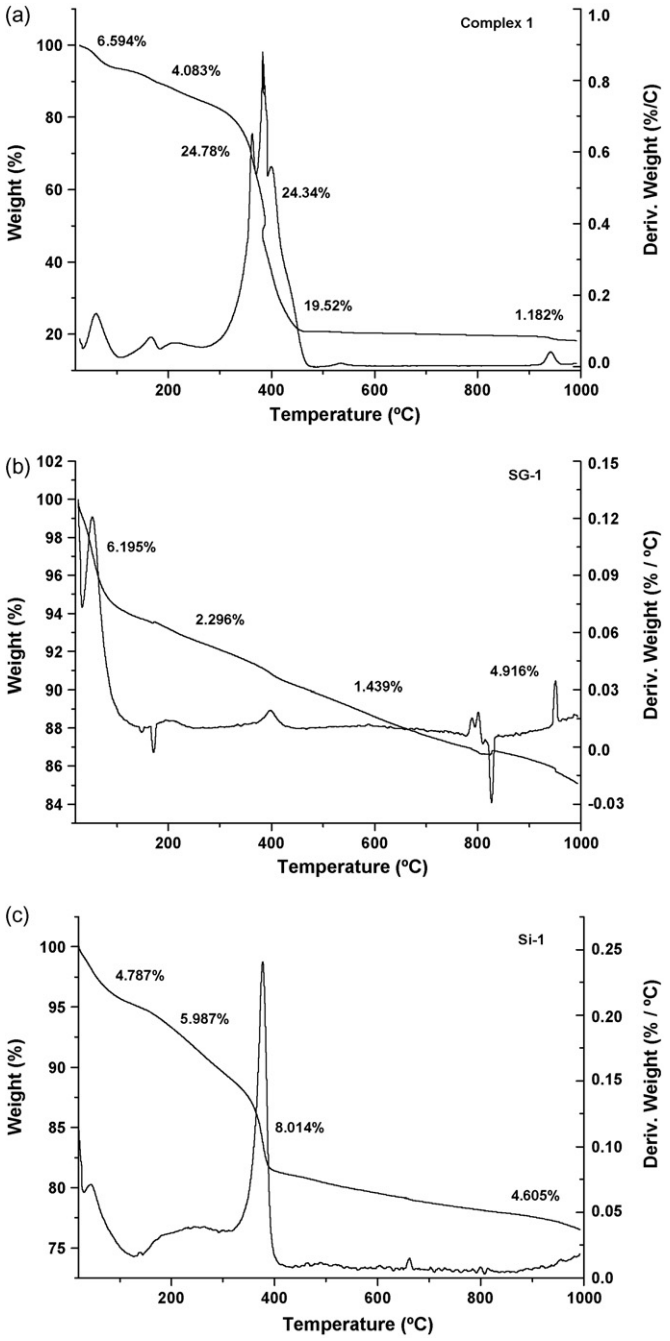

Fig. 3. Thermogravimetric analyses (TGA and DSC) for complex **1** (a), **SG-1** (b), and **Si-1** (c).

3.3. Alkene oxidation

The catalytic activity of **1** in solution (homogeneous catalysis), and immobilized on silica (**Si-1**) or entrapped in a silica matrix by the sol–gel route (**SG-1**) (heterogeneous catalysis) was investigated in the oxidation of cyclooctene and cyclohexene using iodosylbenzene as oxidant. Results are presented in Table 1.

Complex **1** catalyzes the oxidation of cyclooctene and cyclohexene by PhIO in both homogeneous and heterogeneous media (**Si-1** and **SG-1**). Control reactions carried out in the absence of **1** do not give evidence of considerable activity for any of the substrates (oxidized product yields below 6%). All the reactions revealed the selective formation of epoxide, with no allylic products forma-

Table 1
Results obtained in the oxidation of cyclooctene and cyclohexene[a] by iodosylbenzene[b] catalyzed by complex **1** (homogeneous catalysis), and **Si-1** and **SG-1** (heterogeneous catalysis).

Catalyst[b]	Reaction time (h)	Cyclohexene[c]		Cyclooctene[c]	
		Run	Epoxide yield (%)	Run	Epoxide yield (%)
1	1	1	26	7	37
	6	2	33	8	74
Si-1	1	3	39	9	42
	6	4	35	10	36
SG-1	1	5	27	11	29
	6	6	34	12	74

[a] Conditions: reaction vessel purged with argon for 10 min.; substrates: cyclooctene or cyclohexene, solvent (dichloromethane/acetonitrile (1:1)) at room temperature.

[b] Manganese complex/iodosylbenzene/substrate molar ratio = 1:10:1000.

[c] Yields based on starting PhIO. Control experiments yielded about 4–6% cyclooctenoxide in the case of both homogeneous and heterogeneous catalysis, while for cyclohexenoxide the yields were 1.2–3.0% (homogeneous catalysis) and 2.0–4.0% (heterogeneous catalysis).

tion. The product yields (Table 1) obtained in the epoxidation of cyclooctene and cyclohexene by **1** in both homogeneous and heterogeneous systems are similar to those observed by us [40–42] and others for metalloporphyrin systems [43–45]. This suggests that complex **1** is an active catalyst for epoxidation reactions under the conditions reported here.

Even noncatalyzed cyclooctene oxidation processes commonly lead to epoxide as the sole product [8,9,46]. However, noncatalyzed cyclohexene oxidation reactions are poorly selective, leading to major alcohol and ketone production and minor epoxide formation [43]. Despite catalyzed epoxidation reactions can lead to better selectivities even some second and third generation porphyrin-based catalysts, which are considered efficient catalytic systems, can produce epoxide, alcohol and ketone in similar yields [47]. The systems studied in this work are selective for the epoxide in the case of both substrates. These results suggested a metal-oxo intermediate as the catalytically active specie as has generally been proposed for catalytic systems leading to the preferential formation of epoxide [46,48–50].

Recently described non-porphyrinic manganese complexes have shown variable catalytic efficiency in oxidation reactions using iodosylbenzene as oxidant. Mn^{III}(salen) complexes have been extensively studied. Kochi has reported selective cyclohexene epoxidation reactions (36–67% epoxide yields) depending on salen substituents [50]. Nam and co-workers [51] have studied the influence of ligand nature of counterions on the product selectivity. For the Mn(salen)Cl system the epoxide yields (based on the added oxidant) were around 27% for cyclohexene epoxide, similar to the yield obtained in run 1, Table 1. However, their system was not selective because there was formation of allylic products as well (20% yield for cyclohexenol and 29% yield for cyclohexenone). Better results were obtained for Mn(salen)CF_3SO_3 (45% for epoxide). These results suggest that the ligands structures and the metal ion present in the structure of the catalyst complex affect not only catalytic activity but also product distribution in olefin epoxidation reactions.

Chattopadhyay et al. [52] have studied the effect on catalytic efficiency of the presence of a second metal in the vicinity of a Mn(III) center in Mn(III)salen similar complexes. They observed that the second metal (Cu(II), Fe(III), Zn(II), Ni(II), Co(II), Mn(III)) has a detrimental effect on catalyst efficiency in the case of styrene and stylbene epoxidations. These authors demonstrated that, among the binuclear compounds, $Mn^{III}Mn^{III}$ leads to the best results. They attributed the decrease in substrate conversion to a possible PhIO decomposition in the presence of bimetallic complexes, which should result in the formation of unwanted products instead of the PhI and Mn^{V}=O species.

Comparing the catalytic efficiency of the binuclear complex **1** in homogeneous system with those of some recently reported mononuclear manganese complexes coordinated with ligands containing N,O donor sets, used without co-catalysts, the former displays similar catalytic efficiency, but higher selectivity for the epoxide in the case of cyclohexene oxidation by PhIO (epoxide yields around 25–40% based on PhIO) [4,53]. Therefore, factors such as the complete structure of the complex, the distance between the metal centers, and the presence of labile sites to coordination of the oxidant molecule must be considered when the effect of catalyst nuclearity is analyzed.

Table 1 shows that the catalytic results obtained in the presence of complex **1** depend on the reaction conditions. In the case of the reactions carried out for 1 h, all the catalysts (homogeneous complex **1** and heterogeneous **Si-1** and **SG-1**) display similar catalytic performance, leading to epoxide yields ranging between 30 and 42%. When the reaction time is increased to 6 h, differences in the catalytic activities of the three systems become more evident. In the case of the more inert substrate cyclohexene, a longer reaction time does not affect the final yield; there is improvement of around 7% for complex **1** (runs 1 and 2) and **SG-1** (runs 5 and 6), while for **Si-1** the increase in reaction time promotes a decrease in epoxide production (runs 3 and 4). As for cyclooctene, a less inert substrate, longer reaction times result in increasing epoxide yields in the case of complex **1** (37–74%) and **SG-1** (29–74%). As observed for cyclohexene, longer reaction times promote a reduction in product yields in the case of **Si-1**.

Apparently, heterogenization of **1** by its entrapment into silica gel via the sol–gel process does not significantly affect epoxide yields. In most of the conditions, immobilization of **1** does not influence the epoxidation results. Only in the case of the reaction using **Si-1** for 6 h is there a decrease in substrate conversion (36% compared with 74% in homogeneous system, runs 10 and 8, respectively). Considering all the runs, **SG-1** leads to results similar to the ones obtained with **1** in homogeneous solution.

The observed results for heterogeneous catalysis are in the same range of those described for porphyrins and Jacobsen catalysts. The use of entrapped catalysts in zeolite, silica, alumina and other porous solids, in epoxidation of cyclooctene and cyclohexene with PhIO as oxidant, result in a large variety of epoxide yields. Mn^{III}(salen) immobilized in alumina by a sol–gel method promoted the epoxidation of cyclooctene with 16% of cyclooctenoxide yield [54]. Similar results (11%) were obtained by Jacobs for the cyclohexene epoxidation using the same catalyst immobilized in zeolite [55]. Better results were obtained by Mayoral and co-workers using clay-supported Mn^{III}(salen) catalysts (33–64% for epoxidation of cyclohexene) [56].

The epoxide yields obtained using **1** immobilized in silica matrix by sol-gel route are similar to those obtained for iron tetraphenylporphyrin in the same solid and reactions conditions [26] and more selective than the same porphyrin immobilized in porous vycor glass [57].

Attempts were made to use hydrogen peroxide (H_2O_2) and *tert*-butylhydroperoxide (TBHP) as oxidant in homogeneous and heterogeneous media, but products were obtained in lower yields (cyclooctenoxide (1–14%) and cyclohexenoxide (0–4%) after 6 h of reactions) than in the case of PhIO. These low product yields are attributed to the competitive parallel reaction of hydrogen peroxide decomposition promoted by **1** in homogeneous media, and also by the supported systems. This proposal is based on the observation that large quantities of molecular oxygen are produced in all the three reaction systems (homogeneous and heterogeneous), indicating that catalase-like reactions in which the catalytic active

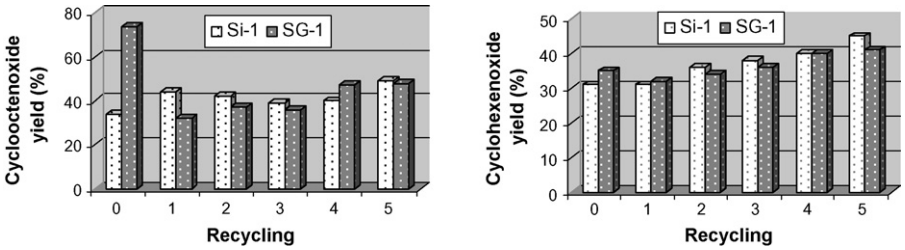

Fig. 4. Recycling studies performed with the **SG-1** and **Si-1** catalysts in the oxidation of cyclooctene and cyclohexene by iodosylbenzene, after 6 h of reaction time.

species could be involved in the decomposition of hydrogen peroxide into molecular oxygen and water through the well described O–O homolysis are taking place [58,59].

Complex **1** is highly stable under the oxidation reaction conditions. In fact, the solution obtained at the end of the homogeneous oxidation reactions were analyzed by UV–vis spectroscopy and they displayed the same bands, with similar intensity, as the starting complex in solution. The immobilized catalyst is also highly stable since no complex or destroyed residues were observed by UV–vis analysis of the reaction solution obtained after the oxidation reaction. In other words, **1** is not leached from the support.

3.4. Catalyst recycling

Product and catalyst separation from the reaction medium still remains troublesome in the case of homogeneous systems [60]. Besides the easier removal of the catalyst from the reaction medium, catalyst reuse is one of the great advantages of heterogeneous catalysis. Therefore, investigating heterogeneous processes is of utmost importance because it can provide insights into the efficiency of the metal complex anchoring process and furnish information on catalyst stability during the catalytic cycle. In order to investigate the possibility of several recycling runs for **Si-1** and **SG-1**, the solid catalysts were separated from the reaction mixture by centrifugation after the reaction, washed exhaustively with methanol and acetonitrile in a Soxhlet extractor for 6 h, dried at room temperature, and used again in a fresh reaction. The catalyst was recycled five times for cyclooctene and cyclohexene epoxidations. In general, no substantial loss in the catalytic activity of the immobilized catalyst was observed compared with that of fresh sample, as shown in Fig. 4. Therefore, recycling is possible in the cases of **Si-1** and **SG-1**.

3.5. In situ spectroscopic and electrochemical studies

To investigate the intermediate active species formed in the reaction between complex **1** and the oxidant, UV–vis spectra of the complex in the presence of PhIO were recorded. After addition of PhIO**,** the color of the solution containing **1** changes to dark brown. The maximum absorbance observed at 470 nm for complex **1** shifts to 486 nm, and there is an increase in the intensity (Fig. 5a). After 40 min, the absorbance returns to the initial level, but the spectrum profile is not the same. Similar results have been reported for manganese(III)–salen complexes [50,61,62], binuclear Mn(II) complexes with Schiff base ligands [4], and Mn–tmtacn complexes [63]. In the presence of cyclohexene, the same behavior is observed (Fig. 5b). However, after 48 h the spectrum is identical to that of the starting complex, indicating that **1** is restored in the solution.

The reactivity of **1** toward PhIO was also accompanied by electrochemical studies. The addition of the oxidant to an acetronitrile solution of **1** promotes a change in the potentials. The wave attributed to the $Mn^{II}Mn^{III} \rightarrow Mn^{III}Mn^{III}$ process disappears, and a new peak occurs at −0.2 V with the corresponding oxidation process at −0.01 V (Fig. 6). Electrochemical processes around the potential observed in these experiment have been attributed to the $Mn^{IV} \rightarrow Mn^{III}$ reduction of manganese coordinated to oxide ligands like Mn=O or Mn–O–Mn sites of well characterized complexes with phenol-Schiff base ligands [64–66].

The changes in oxidation states for the complex in the reaction media were monitored using EPR spectroscopy at 77K. The EPR spectrum of **1** in dichloromethane/acetonitrile (1:1) mixture shows broad features attributed to superimpositions of all the possible spin states ($S = 1/2, 3/2, 5/2, 7/2$ and $9/2$) (Fig. 7a). The spectrum at 10 K (Fig. S2—supplementary material) have shown a characteristic 21-line hyperfine pattern about $g = 2$, arising from $S = 1/2$ ground state, typical of mixed valence center $Mn^{II}Mn^{III}$. Similar signals for others $Mn^{II}Mn^{III}$ complexes have been observed just at very low temperatures [32–35,67].

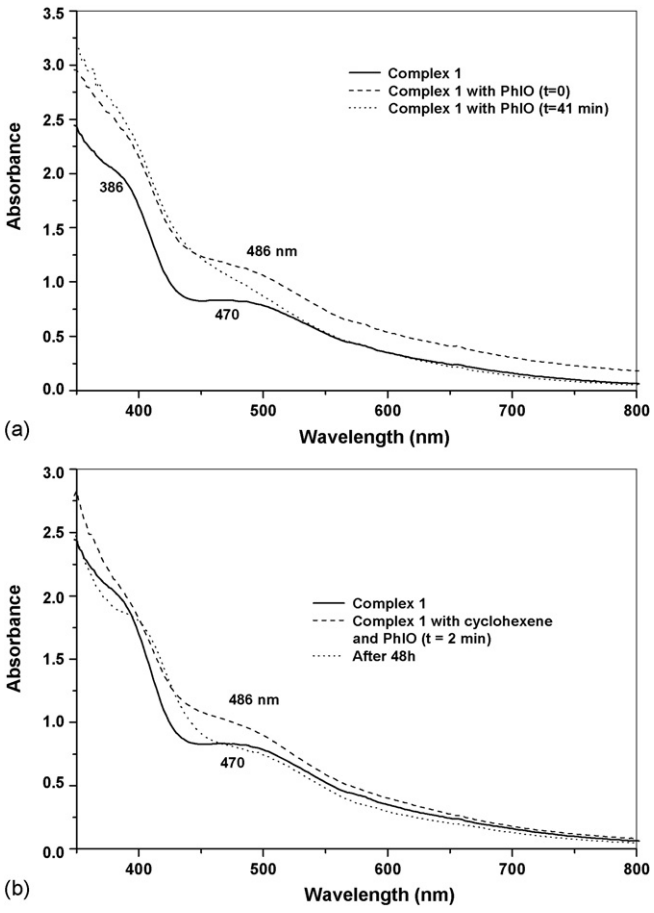

Fig. 5. UV–vis spectra of the reaction media in dichloromethane/acetonitrile/methanol = 0.25:0.25:1. (a) **1**/PhIO molar ratio = 1:10 and (b) **1**/PhIO/cyclohexene molar ratio = 1:10:1000.

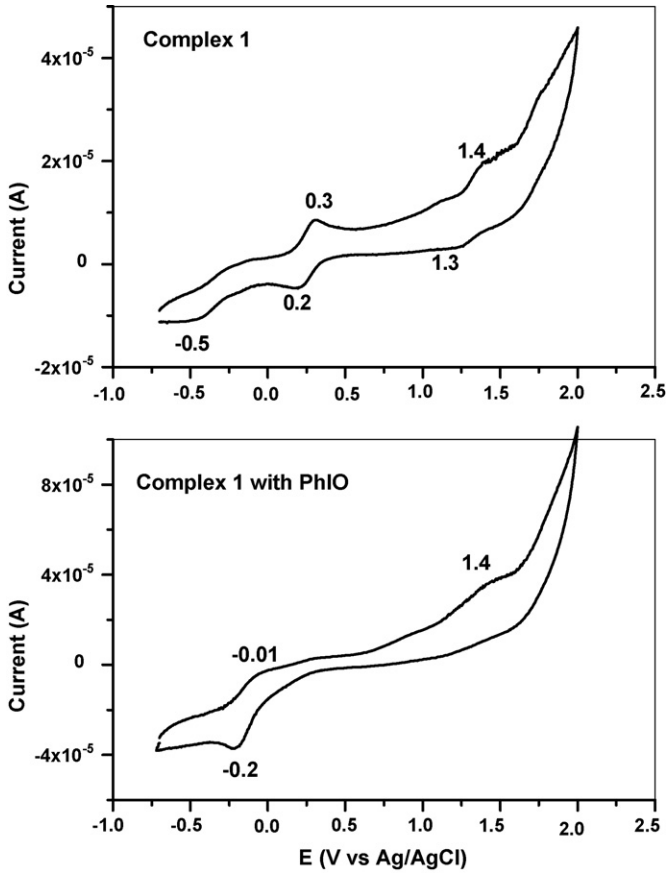

Fig. 6. (a) Cyclic voltammogram of **1** in acetonitrile (1×10^{-3} mol L^{-1}). (b) Cyclic voltammogram of **1** in acetonitrile/methanol (1×10^{-3} mol L^{-1}) after addition of PhIO (1:10). Working electrode: vitreous carbon; Reference electrode: Ag/AgCl; Counter electrode: platinum wire; Supporting electrolyte: $TBAPF_6$ (0.1 mol L^{-1}); Scan rate: 100 mV s^{-1}.

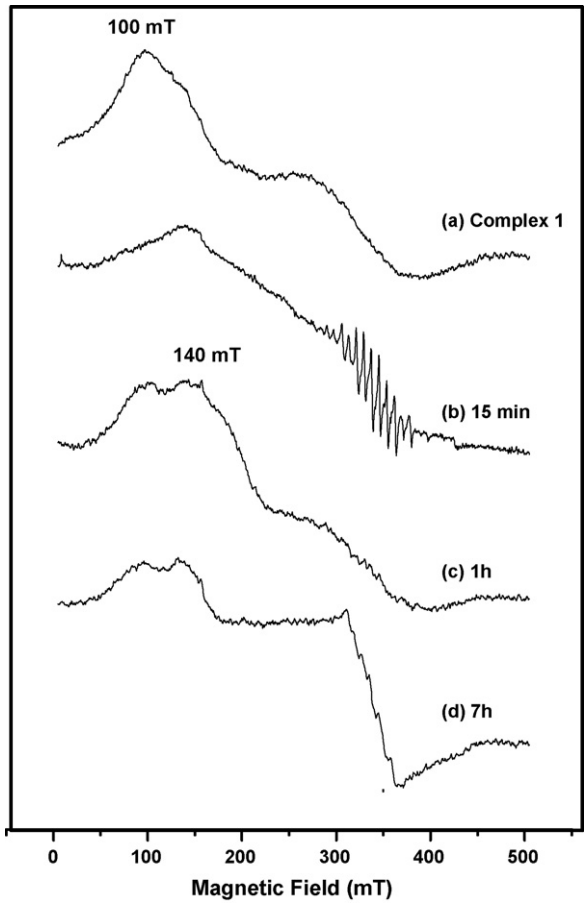

Fig. 7. Time series of the 77K EPR spectra of 1 in dichloromethane/acetonitrile (1:1) mixture after the addition of PhIO in the presence of cyclooctene (1:10:1000 ratio). (a) Just complex **1**; (b–d) after 15 min, 1 h and 7 h. Experimental parameters: microwave frequency, 9.435511 GHz, temperature 77 K, field modulation amplitude, 0.36 mT and microwave power, 20 mW).

The EPR spectrum taken just after addition of PhIO in the presence of cyclooctene (1:10:1000 ratio) lacked the broad features observed before. After 15 min a 16-line hyperfine pattern about $g = 2$ was observed (Fig. 7b), which is consistent to a dinuclear $Mn^{III}Mn^{IV}$ complex with antiferromagnetic spin coupling between the manganese centers [20,36,68–69]. The spectrum was simulated using an effective electron spin $S = 1/2$ arising from antiferromagnetically coupled $Mn^{III}Mn^{IV}$ pair, $S = 2$ and 3/2, respectively (Fig. 8). An effective anisotropic *g*-tensor in agreement to those found in literature [4,70] for the binuclear complex was obtained. Two hyperfine anisotropic *A*-tensors were determined and assigned to the different valence Mn center (Table 2). The best line shape fitting was achieved using gaussian line shapes. Collinear *g* and *A* tensors were used.

The EPR spectra time series (Fig. 7c) from 1 to 6 h showed similar features to the starting complex differing by one additional signal around 140 mT ($g = 4.7$). Adam et al. [71] have attributed signals at *g* ca. 2 and ca. 5 to a Mn^{IV}(salen) species formed by reaction of PhIO with Mn^{III}(salen). The same attributions have also been made by other authors [20]. After 7 h (Fig. 7d) a signal with six hyperfine lines has appeared at $g = 2$ which is typical of mononuclear Mn^{II} species.

As it has been extensively studied by Adam et al. [71], Jacobsen and co-workers [72], Collman et al. [61] and Nam and co-workers [51], Mn^{III}(salen) oxidations reactions with iodosylarenes implies the presence of adducts formed by the manganese complex and the oxidant (Mn^{III}–OIPh) besides the involvement of multiple oxidants in the oxygen transfer. The active specie are considered to be a Mn^{V}=O complex, as proposed by Kochi for porphyrins and Mn(salen) systems [50,61]. Unfortunately Mn^{III} and Mn^{V} species are EPR inactive. The participation of an Mn^{IV}(salen) intermediate has also been evidenced by Adam in systems using dichloromethane as solvent with the formation of $Mn^{IV}OCl$ or Mn^{IV}=O species responsible for chlorine or oxygen transfer [71]. In our system the preferential formation of epoxide and the EPR spectra leads

Table 2
Simulated giromagnetic and hyperfine couplings for the $Mn^{III}Mn^{IV}$ specie formed by reaction of **1** with PhIO at 77 K.

	Hyperfine couplings (mT)				Effective giromagnetic couplings				Line width (mT)
	A_x	A_y	A_z	A_{iso}	g_x	g_y	g_z	g_{iso}	
Mn(III)	16.582	15.474	9.7499	13.935	2.00747	2.00382	1.98308	1.99813	2.1992
Mn(IV)	8.3618	8.0749	7.8506	8.0957					

g_{iso} refers to the average $g_{iso} = (g_x + g_y + g_z)/3$ and similarly is $A_{iso} = (A_x + A_y + A_z)/3$.

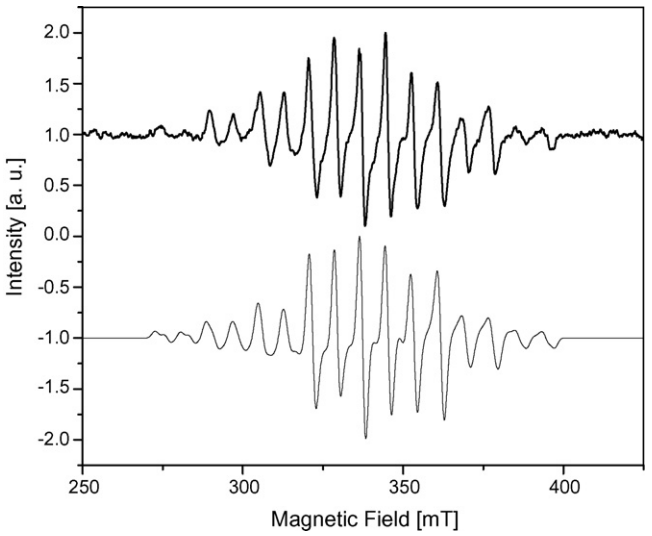

Fig. 8. Experimental (thick line) and simulated (thin line) frozen solution spectra of $Mn^{III}Mn^{IV}$ binuclear complex. Experimental parameters: microwave frequency, 9.435511 GHz, temperature 77 K, field modulation amplitude, 0.36 mT, microwave power, 20 mW, conversion time, 655.36 ms per point, time constant, 2.62 s, 2048 resolution points.

us to expect the Mn^{V}=O, Mn^{IV}=O or Mn^{III}–OIPh intermediates species as observed for various porphyrin and non-porphyrin complexes [51,61,63,71–75]. The lability of the bridging acetate groups may afford vacant coordination points for the oxygen atom. The observed dinuclear $Mn^{III}Mn^{IV}$ specie may be formed by intramolecular electron transfer from the arising Mn^{V} to Mn^{II} center leading to an unreactive μ-oxo complex. A similar mechanism was proposed to Mn(salen) by Kochi [50] and to others dinuclear systems in oxidation reactions.

4. Conclusions

The heptadentate ligand H_3bbppnol, which has an alcohol group between the nitrogen atoms of the propanediamine, promotes the formation of a binuclear manganese compound. The characterization of this complex indicates the structural formula $[Mn^{II}Mn^{III}(bbppnol)(\mu\text{-}OOCCH_3)_2]$.

The accessibility of various redox states observed by the electrochemical characterization motivated the use of this complex as catalyst for alkene oxidation reactions in both homogeneous and heterogeneous media.

The catalytic study reveals that the complex performs well as epoxidation catalyst. The solids containing the immobilized complex can be successfully removed from the reaction media and recycled.

Acknowledgements

The authors are grateful to Conselho Nacional de Desenvolvimento Científico e Tecnológico (CNPq), Coordenação de Aperfeiçoamento de Pessoal de Nível Superior (CAPES), Fundação Araucária, and Universidade Federal do Paraná (UFPR) for financial support.

Appendix A. Supplementary data

Supplementary data associated with this article can be found, in the online version, at doi:10.1016/j.molcata.2008.10.037.

References

[1] E.M. McGarrigle, D.G. Gilheany, Chem. Rev. 105 (2005) 1563–1602.
[2] H.U. Blaser, B. Pugin, F. Spindler, J. Mol. Catal. A: Chem. 231 (2005) 1–20.
[3] G.B. Shul'pin, J. Mol. Catal. A: Chem. 189 (2002) 39–66.
[4] C.A. Sureshan, P.K. Bhattacharya, J. Mol. Catal. A: Chem. 136 (1998) 285–291.
[5] C.M. Che, J.S. Huang, Coord. Chem. Rev. 242 (2003) 97–113.
[6] W. Nam, H.J. Kim, S.H. Kim, R.Y.N. Ho, J.S. Valentine, Inorg. Chem. 35 (1996) 1045–1049.
[7] Y.N. Ito, T. Katsuki, Bull. Chem. Soc. Jpn. 72 (1999) 603–619.
[8] C. Piovezan, K.A.D.F. Castro, S.M. Drechsel, S. Nakagaki, Appl. Catal. A: Gen. 28 (2005) 97–104.
[9] S. Nakagaki, F. Wypych, M. Halma, F.L. Benedito, G.R. Friedermann, A. Bail, G.S. Machado, S.M. Drechsel, Met. Mater. Process 17 (2005) 363–380.
[10] J.R. Lindsay-Smith, B.C. Gilbert, A.M. Payeras, J. Murray, T.R. Lowdon, J. Oakes, R.P. Prats, P.W. Walton, J. Mol. Catal. A: Chem. 251 (2006) 114–122.
[11] G.B. Shul'pin, G. Suss-Fink, L.S. Shul'pin, J. Mol. Catal. A: Chem. 170 (2001) 17–34.
[12] C.B. Woitiski, Y.N. Kozlov, D. Mandelli, G.V. Nizova, U. Schuchardt, G.B. Shul'pin, J. Mol. Catal. A: Chem. 222 (2004) 103–119.
[13] K. Wieghardt, U. Bossek, B. Nuber, J. Weiss, J. Bonvoisin, M. Corbella, S.E. Vitols, J.J. Girerd, J. Am. Chem. Soc. 110 (1988) 7398–7411.
[14] D.E. De Vos, B.F. Sels, M. Reynaers, Y.V. Subba Rao, P.A. Jacobs, Tetrahedron Lett. 39 (1998) 3221–3224.
[15] D.E. De Vos, P.A. Jacobs, Catal. Today 57 (2000) 105–114.
[16] J. Brinksma, L. Schmieder, G. van Vliet, R. Boaron, R. Hage, D.E. De Vos, P.L. Alsters, B.L. Feringa, Tetrahedron Lett. 43 (2002) 2619–2622.
[17] J. Brinksma, R. Hage, J. Kerschner, B.L. Feringa, Chem. Commun. (2000) 537–538.
[18] J.H. Koek, E.W.M.J. Kohlen, S.W. Russel, L. Van Der Wolf, P.F. Steeg, J.C. Hellemons, Inorg. Chim. Acta 295 (1999) 189–199.
[19] J.W. De Boer, J. Brinksma, W.R. Browne, A. Meetsma, P.L. Alsters, R. Hage, B.L. Feringa, J. Am. Chem. Soc. 127 (2005) 7990–7991.
[20] M.T. Caudle, P. Riggs Gelasco, A.K. Gelasco, J.E. Penner Hahn, V.L. Pecoraro, Inorg. Chem. 35 (1996) 3577–3584.
[21] A. Neves, S.M. Drechsel Erthal, V. Drago, K. Griesar, W. Haase, Inorg. Chim. Acta 197 (1992) 121–124.
[22] W. Stober, A. Fink, J. Colloid Interf. Sci. 26 (1968) 62–69.
[23] J.G. Sharefkin, H. Saltzmann, Org. Synth. 43 (1963) 62–64.
[24] J. Lucas, E.R. Kennedy, M.W. Forno, Org. Synth. 22 (1955) 70–71.
[25] S. Stoll, A. Schweiger, J. Magn. Reson. 178 (2006) 42–55.
[26] A.T. Papacídero, L.A. Rocha, B.L. Caetano, E. Molina, H.C. Sacco, E.J. Nassar, Y. Martinelli, C. Mello, S. Nakagaki, K.J. Ciuffi, Coll. Surf. A: Physicochem. Eng. Aspects 275 (2006) 27–35.
[27] W.J. Geary, Coord. Chem. Rev. 7 (1971) 81–122.
[28] K. Nakamoto, Infrared and Raman Spectra of Inorganic and Coordination Compounds, 5th ed., 1970.
[29] A. Neves, S.M.D. Erthal, I. Vencato, A.S. Ceccato, Y.P. Mascarenhas, O.R. Nascimento, M. Hörner, Inorg. Chem. 31 (1992) 4749–4751.
[30] A. Neves, S.M. Drechsel Erthal, I. Vencato, Inorg. Chim. Acta 262 (1997) 77–80.
[31] A. Magnuson, P. Liebisch, J. Högblom, M.F. Anderlund, R. Lomoth, W. Meyer-Klaucke, M. Haumann, H. Dau, J. Inorg. Biochem. 100 (2006) 1234–1243.
[32] H. Diril, H.-R. Chang, X. Zhang, S.K. Larsen, J.A. Potenza, C.G. Pierpont, H.J. Schugar, S.S. Isted, D.N. Hendrickson, J. Am. Chem. Soc. 109 (1987) 6207–6208.
[33] R.M. Buchanan, K.J. Oberhauser, J.F. Richardson, Inorg. Chem. 27 (1988) 973–974.
[34] H.R. Chang, H. Diril, M.J. Nilges, X. Zhang, J.A. Potenza, H.J. Schugar, D.N. Hendrickson, S.S. Isied, J. Am. Chem. Soc. 110 (1988) 625–627.
[35] M. Suzuki, M. Mikuriva, S. Murata, A. Uehara, H. Oshio, S. Kida, K. Saito, Bull. Chem. Soc. Jpn. 60 (1987) 4305–4312.
[36] L. Dubois, R. Caspar, L. Jacquamet, P.-E. Petit, M.F. Charlot, C. Baffert, M.-N. Collomb, A. Deronzier, J.-M. Latour, Inorg. Chem. 42 (2003) 4817–4827.
[37] H. Diril, H.R. Chang, M.J. Nilges, X. Zhang, J.A. Potenza, H.J. Schugar, S.S. Isied, D.N. Hendrickson, J. Am. Chem. Soc. 111 (1989) 5102–5114.
[38] R. Lomoth, P. Huang, J. Zheng, L. Sun, L. Hammarström, B. Akermark, S. Styring, Eur. J. Inorg. Chem. 2002 (2002) 2965–2974.
[39] C.C. Perry, X. Li, D.N. Waters, Spectrochim. Acta 47A (1991) 1487–1494.
[40] A.M. Machado, F. Wypych, S.M. Drechsel, S. Nakagaki, J. Colloid Interf. Sci. 254 (2002) 158–164.
[41] M. Halma, F. Wypych, S.M. Drechsel, S. Nakagaki, J. Porphyr. Phthalocya. 6 (2002) 502–513.
[42] S. Nakagaki, K.A.D.F. Castro, G.S. Machado, M. Halma, S.M. Drechsel, F. Wypych, J. Braz. Chem. Soc. 17 (2006) 1672–1678.
[43] S. Tanase, C. Foltz, R. Gelder, R. Hage, E. Bouwman, J. Reedijk, J. Mol. Catal. A: Chem. 225 (2005) 161–167.
[44] J. Haber, J. Iwanejko, P. Battioni, R. Mansuy, J. Mol. Catal. A: Chem. 152 (2000) 111–115.
[45] A.J. Appleton, S. Evans, J.R. Lindsay-Smith, J. Chem. Soc. Perkin Trans. 2 (1996) 281–285.
[46] Y. Suh, M.S. Seo, K.M. Kim, Y.S. Kim, H.G. Jang, T. Tosha, T. Kitagawa, J. Kim, W. Nam, J. Inorg. Biochem. 100 (2006) 627–633.
[47] E. Nascimento, G.F. Silva, F.A. Caetano, M.A.m. Fernandes, D.C. da Silva, M.E.M.D. Carvalho, J.M. Pernaut, J.S. Rebouças, Y.M. Idemori, J. Inorg. Biochem. 99 (2005) 1193–1204.
[48] D. Mansuy, Pure Appl. Chem. 62 (1990) 741–746.
[49] T.G. Traylor, Pure Appl. Chem. 63 (1991) 265–274.
[50] K. Srinivasan, P. Michaud, J.K. Kochi, J. Am. Chem. Soc. 108 (1986) 2309–2320.

[51] S.E. Park, W.J. Song, Y.O. Ryu, M.H. Lim, R. Song, K.M. Kim, W. Nam, J. Inorg. Biochem. 99 (2005) 424–431.
[52] T. Chattopadhyay, S. Islam, M. Nethaji, A. Majee, D. Das, J. Mol. Catal. A: Chem. 267 (2007) 255–264.
[53] O. Pouralimardan, A.C. Chamayou, C. Janiak, H. Hosseini-Monfared, Inorg. Chim. Acta 360 (2007) 1599–1608.
[54] T.C.O. Mac Leod, D.F.C. Guedes, M.R. Lelo, R.A. Rocha, B.L. Caetano, K.J. Ciuffi, M.D. Assis, J. Mol. Catal. A: Chem. 259 (2006) 319–327.
[55] P.-P. Knops-Gerrits, D.E. de Vos, P.A. Jacobs, J. Mol. Catal. A: Chem. 117 (1997) 57–70.
[56] J.M. Fraile, J.I. García, J. Massam, J.A. Mayoral, J. Mol. Catal. A: Chem. 136 (1998) 47–57.
[57] S. Nakagaki, A.R. Ramos, F.L. Benedito, P.G. Peralta-Zamora, A.J.G. Zarbin, J. Mol. Catal. A: Chem. 185 (2002) 203–210.
[58] L.R. Guilherme, S.M. Drechsel, F. Tavares, C.J. Cunha, S.T. Castaman, S. Nakagaki, I. Vencato, A.J. Bortoluzzi, J. Mol. Catal. A: Chem. 269 (2007) 22–29.
[59] D. Dolphin, T.D. Traylor, L.Y. Xie, Acc. Chem. Res. 30 (1997) 251–259.
[60] R.I. Kureshy, N.H. Khan, S.H.R. Abdi, S. Singh, I. Ahmad, R.V. Jasra, A.P. Vyas, J. Catal. 224 (2004) 229–235.
[61] J.P. Collman, L. Zeng, J.I. Brauman, Inorg. Chem. 43 (2004) 2672–2679.
[62] B. Bahramian, V. Mirkhani, S. Tangestaninejad, M. Moghadam, J. Mol. Catal. A: Chem. 244 (2006) 139–145.
[63] T.H. Bennur, S. Sabne, S.S. Deshpande, D. Srinivas, S. Sivasanker, J. Mol. Catal. A: Chem. 185 (2002) 71–80.
[64] G.C. Dailey, C.P. Horwitz, C.A. Lisek, Inorg. Chem. 31 (1992) 5325–5330.
[65] C.P. Horwitz, P.J. Winslow, J.T. Warden, C.A. Lisek, Inorg. Chem. 32 (1993) 82–88.
[66] J.W. Gohdes, W.H. Armstrong, Inorg. Chem. 31 (1992) 368–373.
[67] L. Dubois, D.-F. Xiang, X.-S. Tan, J. Pecaut, P. Jones, S. Baudron, L. Le Pape, J.-M. Latour, C. Baffert, S. Chardon-Noblat, M.-N. Collomb, A. Deronzier, Inorg. Chem. 42 (2003) 750–760.
[68] K.S. Hagen, W.H. Armstrong, H. Hope, Inorg. Chem. 27 (1988) 967–969.
[69] K.-O. Schäfer, R. Bittl, W. Zweygart, F. Lendzian, G. Haselhorst, T. Weyhermüller, K. Wieghardt, W. Lubitz, J. Am. Chem. Soc. 120 (1998) 13104–13120.
[70] K.O. Schäfer, R. Bittl, F. Lendzian, V. Barynin, T. Weyhermuller, K. Wieghardt, W. Lubitz, J. Phys. Chem. B 107 (2003) 1242–1250.
[71] W. Adam, C. Mock-Knoblauch, C.R. Saha-Möller, M. Herderich, J. Am. Chem. Soc. 122 (2000) 9685–9691.
[72] M. Palucki, N.S. Finney, P.J. Pospisil, M.L. Güler, T. Ishida, E.N. Jacobsen, J. Am. Chem. Soc. 120 (1998) 948–954.
[73] K.P. Bryliakov, O.A. Kholdeeva, M.P. Vanina, E.P. Talsi, J. Mol. Catal. A: Chem. 178 (2002) 47–53.
[74] J.A. Smegal, C.L. Hill, J. Am. Chem. Soc. 105 (1983) 3515–3521.
[75] A. Martinez, C. Hemmert, H. Gornitzka, B. Meunier, J. Organ. Chem. 690 (2005) 2163–2171.